History of stellar evolution at high redshifts: Implications for the CMB E-mode polarization

L.A. Popa *

INAF/IASF, Istituto di Astrofisica Spaziale e Fisica Cosmica Bologna, I-40129, Italy
ISS, Institute for Space Sciences Bucharest, R-76900, Romania

The epoch of the end of reionization and the Thomson optical depth to the cosmic microwave background depend on the power spectrum amplitude on small scales and on the ionizing photon emissivity per unit mass in collapsed halos. In this paper is investigated the role of the radiative feedback effects for the temporal evolution of the ionizing emissivity.
It is shown that the observational constrains on hydrogen photo-ionization rate based on Ly-α, Ly-β and Ly-γ Gunn-Peterson troughs and an electron optical depth consistent with the latest CMB measurements requires an emissivity of $\sim$10 ionizing photons per baryon and Hubble time at $z = 6$.
Through E-mode CMB polarization power spectrum measurements, is expected that PLANCK experiment will have the sensitivity to distinguish between different histories of stellar evolution.

1. Introduction

The detailed study of the intergalactic medium (IGM) is fundamentally important for understanding the large-scale structure properties and the galaxy formation process.
At the epoch of reionization the collapsed objects began to influence the diffuse gas in the IGM rendered it transparent to the ultraviolet photons. In order to virialize in the potential wells of the dark matter halos, the gas in the IGM must have a mass greater than the Jeans mass $M_J \sim 10^5 M_\odot$ at a redshift $z \sim 30$, corresponding to a virial temperature of $T_{vir} \sim 10^4$K. Photoionization by the high-redshift UV radiation background (UVB) heats the low density gas in the IGM before it falls into the dark matter wells, strongly reducing the fraction of neutral hydrogen and helium that dominate the cooling of the primordial gas at temperatures of T_{vir}.

Reionization is an inhomogeneous process that proceeds in a patchy way. The radiation output associated with the collapsed halos gradually builds up a cosmic UVB. At early times, most of the gas in the IGM is still neutral and the cosmological H_{II} regions around the individual sources do not overlap. At this early stage the gas in the IGM is opaque to the ionization photons, causing fluctuations of both ionization fraction and UVB intensity from region to region. At the reionization redshift the H_{II} regions surrounding the individual sources in the IGM overlap. During reionization, the number of ionizing photons reaching IGM had to be sufficient to ionize every atom in the universe and to balance the recombination.

From the observational point of view, the study of the reionization process itself as well as the properties of the sources driving it is challenged by a variety of observational probes. A powerful observational probe comes from the Lyα absorbtions spectra of the high redshift quasars (Becker et al., 2001, Fan et al., 2002, White et al., 2003, Fan et al., 2004) showing that all known quasars with $z > 6$ have a complete Gunn-Peterson (GP) trough and a rapid evolving hydrogen neutral fraction compatible with the final stage of reionization. An other powerful observational probe is represented by the high value of the electron scattering optical depth τ inferred from the Cosmic Microwave Background (CMB) anisotropy measured by the WMAP experiment (Kogut et al., 2003; Spergel et al., 2003; Verde et al., 2003) which requires reionization to begin at $z > 14$.

In this paper we study the temporal evolu-

tion of the ionizing emissivity in the presence of the radiative transfer effects by using N-body cosmological hydrodinamical simulations at subgalactic scales. Detailed discussion of the simulations can be found in Popa, Burigana, Mandolesi, 2005 (hereafter PBM). Throughout it is assumed a background cosmology consistent with the most recent cosmological measurements (Spergel et al., 2003) with energy density of $\Omega_m = 0.27$ in matter, $\Omega_b = 0.044$ in baryons, $\Omega_\Lambda = 0.73$ in cosmological constant, a Hubble constant of H_0=72 km s^{-1}Mpc^{-1}, an *rms* amplitude of $\sigma_8 = 0.84$ for mass density fluctuations in a sphere of radius 8h^{-1}Mpc, adiabatic initial conditions and a primordial power spectrum with a power-law scalar spectral index $n_s = 1$.

2. Radiative transfer

The cumulative UV background flux, $J(\nu_o, z_o)$, observed at the frequency ν_o and redshift z_o, (in units of 10^{-21} erg cm^{-2} s^{-1} sr^{-1}) due to photons emitted from redshifts between z_o and an effective emission screen located at $z_{sc} \geq z_o$, is the solution of the cosmological radiative transfer equation (Peebles, 1993; Haiman, Rees & Loeb, 1997):

$$J(\nu_o, z_o) = \frac{c}{4\pi} \int_{z_o}^{z_{sc}} e^{-\tau_{eff}(\nu_o, z_o, z)} \frac{dt}{dz} j(\nu_z, z) dz \quad (1)$$

where: $j(\nu_z, z)$ is the comoving emission coefficient (in units of 10^{-21} erg cm^{-3} s^{-1} sr^{-1}) computed at emission redshift z and photon frequency $\nu_z = \nu_o(1+z)/(1+z_o)$, $\tau_{eff}(\nu_o, z_o, z)$ is the effective optical depth at the frequency ν_o due to the absorption of the residual gas in the IGM between z_o and z and $(dt/dz)^{-1} = -H_0(1+z)\sqrt{\Omega_m(1+z)^3 + \Omega_\Lambda}$ is the line element in the ΛCDM cosmology.

Above the hydrogen ionization threshold the UV radiation background is processed due to the absorption of residual gas in the IGM dominated by neutral hydrogen and helium. At these frequencies the effective optical depth is given by (see e.g. Haiman, Rees & Loeb, 1997):

$$\tau_{eff}(\nu_o, z_o, z) = c \int_{z_o}^{z} \frac{dt}{dz} \kappa(\nu_z, z) dz, \quad (2)$$

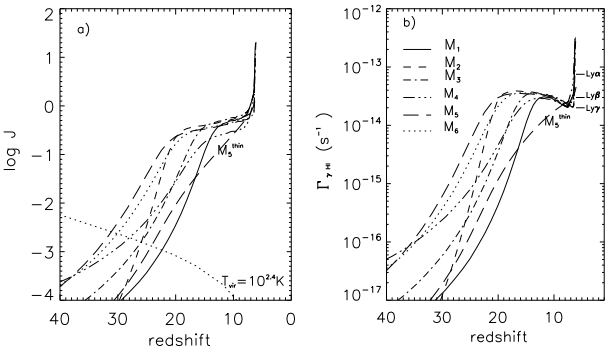

Figure 1. Left panel: Evolution with redshift of the UVB flux at ≈1 Ryd. The critical UVB flux below which ($T_{vir} \leq 10^{2.4}$K) the star formation is prevented (thick dotted line) is from Haiman, Abel & Rees (2000). Right panel: Redshift evolution of the hydrogen photo-ionization rate for the UVB models presented in the right panel. The observational upper limits based on Lyα, Lyβ and Lyγ Gunn-Peterson troughs at $z = 6.05$ are from Fan et al. (2002).

$$\kappa(\nu_z, z) = \sum_i \sigma_i(\nu_z) n_i(z)\,,$$

where: $i = (H_I\,, He_I)$ and σ_i and n_i are the cross section and the number density respectively, corresponding to species i.

The hydrogen photo-ionization rate, $\Gamma_{\gamma_{H_I}}(z)$, is related to the UVB flux, $J(\nu, z)$, through:

$$\Gamma_{\gamma_{HI}}(z) = \int_{\nu_{H_I}}^{\infty} \frac{J(\nu, z)\sigma_{H_I}(\nu)}{h\nu} d\nu \quad (3)$$

where $\sigma_{H_I}(\nu)$ is the hydrogen photo-ionization (dissociation) cross-section (Abel et al. 1997) and ν_{H_I} is the hydrogen ionizing threshold frequency (ν_{H_I} ≈1Ryd).

Figure 1 presents (left panel) the evolution with redshift of the UVB flux at ≈ 1Ryd obtained for different UVB spectrum models (PBM) that constraint the hydrogen photo-ionization rate at $z \simeq 6$ to $\Gamma_{\gamma_{HI}} \simeq 8{\times}10^{-14}$ s^{-1} (right panel) as indicated by the observational upper limits based on Lyα, Lyβ and Lyγ Gunn-Peterson troughs (Fan et al. 2002). In Figure 2 are presented

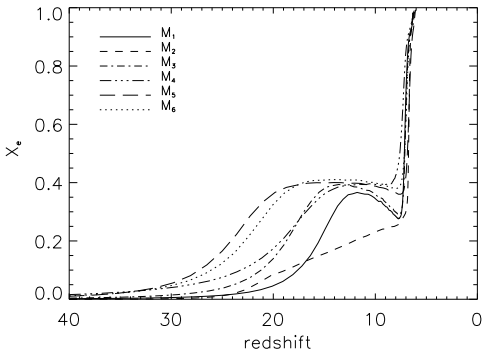

Figure 2. The evolution with redshift of the ionization fraction obtained for the UVB models presented in Figure 1 with electron optical depths τ_{es}=0.05 - 0.1 (PBM).

the corresponding ionization histories with optical depths in the range τ_{es}=0.05 - 0.1 (PBM).
The main effect of the UV radiation spectrum on the temporal evolution of the ionization fraction is given by the value of the reionization redshift and the redshift interval in which the reionization is completed. As reionization proceeds, the radiative feedback raises the Jeans mass in the ionized regions, suppressing the formation of low mass systems. The net effect is a decrease of the global ionization fraction with cosmic time over a limited period.

3. Emissivity evolution

The hydrogen photo-ionization rate is related to the ionizing emissivity, $\epsilon_{H_I}(\nu, z)$ through:

$$\Gamma_{\gamma_{H_I}}(z) = \int_{\nu_{H_I}}^{\infty} d\,\nu \epsilon_{H_I}(\nu, z), \lambda(\nu, z)\sigma_{H_I}(\nu)\,, \quad (4)$$

where $\lambda(\nu, z)$ is the mean free path of the ionizing photons. Assuming $\sigma_{H_I}(\nu) \sim \nu^3$, then $\lambda(\nu, z)$ can be written as (Miralda-Escudé, 2003):

$$\lambda(\nu, z) = \lambda_0 \left(\frac{\nu}{\nu_{H_I}}\right)^{1.5}, \quad (5)$$

where $\lambda_0^{-1}(z)$, the absorbtions probability per unit length for a photon at $\nu = \nu_{H_I}$, is given by:

$$\lambda_0^{-1}(z) = \frac{\sqrt{\pi}}{\lambda_{LL}}, \;\; \lambda_{LL} = cH^{-1}(z)\left(\frac{dN_{LL}}{dz}\right)^{-1}, \quad (6)$$

with $H(z) = H_0\sqrt{\Omega_m(1+z)^3 + \Omega_v}$.
In the above equation dN_{LL}/dz is the Lyman limit system abundance per unit redshift interval. Storrie-Lombardi et al. (1994) found $dN_{LL}/dz = 3.3 \pm 0.6$ at z=4 while Madau, Haardt & Rees (1999) report a value 1.5 times larger (see also Miralda-Escudé, 2003 and references therein).

The mean ionizing emissivity integrated over frequency, expressed as the number of ionizing photons per baryon and Hubble time, can be written as:

$$\frac{\epsilon(z)}{H(z)n_b} = \frac{\sqrt{\pi}}{c}\frac{dN_{LL}}{dz}\int_{\nu_{H_I}}^{\infty}\frac{J(\nu, z)}{h\nu}\left(\frac{\nu}{\nu_{H_I}}\right)^{-1.5} d\nu, \quad (7)$$

where $n_b = 2.07 \times 10^{-7}(\Omega_b h^2/0.022)(1+z)^3 \mathrm{cm}^{-3}$ is the total number density of baryons.
Figure 3 presents the evolution with redshift of the mean ionizing emissivity obtained for various reionization histories.
Figure 4 presents the dependence of the mean ionizing emissivity on the circular velocity and on the virial mass. For all cases, the experimental constraint on hydrogen photo-ionization rate predicts ∼10 ionizing photons per baryon and Hubble time at at $z = 6$. The electron optical depth of τ_{es} =0.05 - 0.1 requires a mean ionizing emissivity of earlier low-mass halos (virial mass of $\sim 10^6 M_\odot$) of order unity.
The emissivity of halos at z =6 ($v_{circ} \approx$50 kms^{-1}) is ∼35 photons as obtained by dividing the mean emissivity of 10 photons per baryon and Hubble time by the baryon collapse fraction (see Figure 5):

$$F_b(z) = x_e f_{coll}(z, T_h) + (1 - x_e) f_{coll}(z, T_c)\,, \quad (8)$$

where $f_{coll}(z, T_h)$ and $f_{coll}(z, T_c)$ are the collapse fractions for the regions with the temperature higher than the virial temperatures $T_h = 2.5 \times 10^4$K and $T_c = 10^{2.4}$K (Haiman, Abel & Rees, 2000; Barkana & Loeb, 2001).
In Figure 5 these numbers are compared with the number of photons that can be produced by star formation assuming that N_γ=2.5×10^4 photons

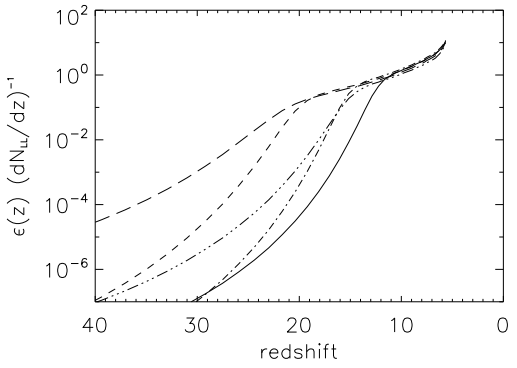

Figure 3. Evolution with redshift of the mean ionizing emissivity (number of ionizing photons per baryon and Hubble time) corresponding to the reionization histories presented in Figure 2.

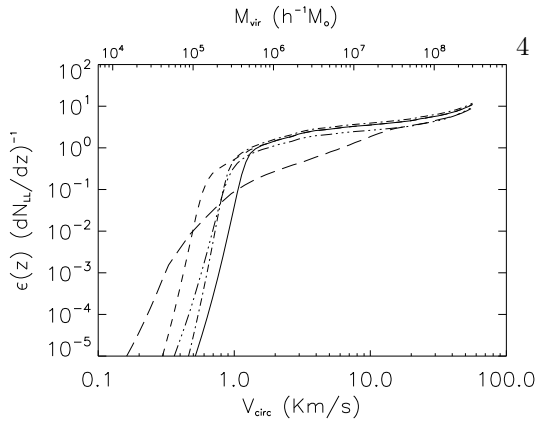

Figure 4. Dependence on circular velocity (virial mass) of the mean ionizing emissivity corresponding to the reionization histories presented in Figure 2.

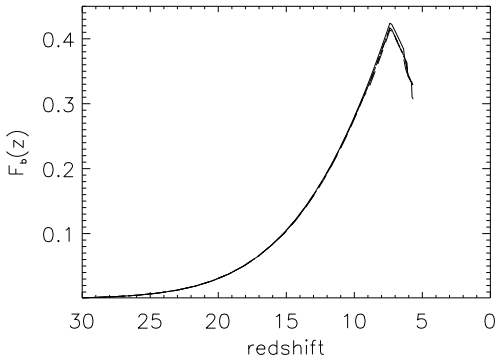

Figure 5. Fraction of mass collapsed into halos as function of redshift.

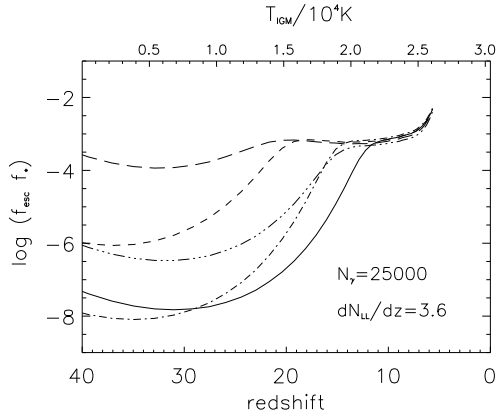

Figure 6. Evolution with redshift and IGM temperature of the product $f_{esc}f_*$ corresponding to the reionization histories presented in Figure 2.

per baryon are emitted by zero-metalicity stars with $M > 20M_\odot$ (Onken & Miralda-Escude, 2004) and $dN_{LL}/dz = 3.6$ (Storrie-Lombardi et al. 1994). If f_* is the fraction of the gas in halos that can be converted into stars with $M > 20M_\odot$ and f_{esc} is the fraction of the photons that escape into IGM, then the experimental constraint on $\Gamma_{\gamma_{HI}} \simeq 8{\times}10^{-14}\mathrm{s}^{-1}$ requires $f_{esc}f_* \approx 10^{-1.9}$ at $z = 6$.
The electron optical depth τ_{es} =0.05 - 0.1 predicts $f_{esc}f_* = 10^{-2.7} - 10^{-1.9}$ for z =15 - 6.
This values comparable with $f_{esc}f_* >(10^{-2.4},10^{-2.8})$ found by Onken & Miralda-Escudé (2004) for the same population of stars by using an analytical model normalized to 7 photons per baryon and Hubble time at $z = 4$ and requiring τ_{es}=0.17 (Miralda-Escudé 2003).

4. Implications for the CMB E-mode polarization

The CMB anisotropy temperature, $C_T(l)$, and E-mode polarization, $C_E(l)$, power spectra corresponding to the various ionization histories are presented in Figure 6.
While $C_T(l)$ power spectra are almost degenerated, the differences in different reionization histories produce undegenerated signatures on $C_E(l)$ power spectra at low multipoles ($l \leq 50$). This

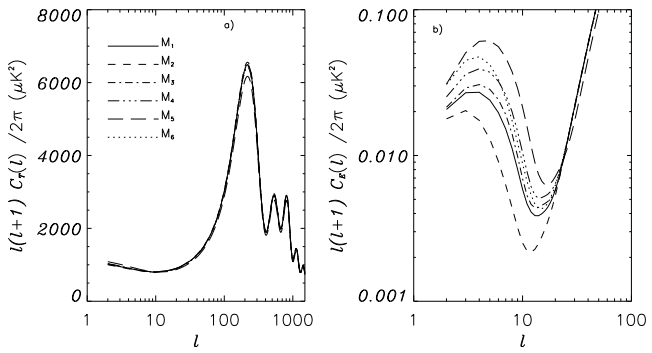

Figure 7. The CMB angular power spectra, $C_T(l)$ and $C_E(l)$ for the reionization histories presented in Figure 2.

can be explained by the fact that while polarization is projecting from the epoch of reionization at angular frequencies $l = k(\eta_0 - \eta_{ri})$ (here k is the wave number, η_0 and η_{ri} are the conformal times today and at the epoch of reionization) the temperature is projecting from the (further) last scattering surface.

It is expected that through E-mode CMB polarization power spectrum measurements, the PLANCK experiment will have the sensitivity to distinguish between different histories of stellar evolution even they imply the same optical depth to electron scattering and degenerated C_T power spectra (PBM).

REFERENCES

1. Abel, T., Anninos, P., Zhang, Y., Norman, M.L., 1997 , NewA 2, 181.
2. Barkana, R., Loeb, A. 2001. Physics Reports 349, 125.
3. Becker, R.H. et al. 2001. ApJ 122, 2850.
4. Fan, X. et al. 2002. AJ, 123, 1247.
5. Fan, X. et al. 2004, AJ 128, 515.
6. Haiman, Z., Abel, T., Rees, M., 2000. ApJ 534, 11.
7. Kogut, A. et al. 2003. ApJS 148, 161.
8. Miralda-Escudé, J., 2003. ApJ 597, 66.
9. Madau, P., Haardt, F., & Rees, M.J. , 1999. ApJ 514, 648.
10. Naselsky, P., Chiang, L.Y., 2004. MNRAS, 347, 795.
11. Onken, C.A., Miralda-Escudé, J., 2004. ApJ 610, 1.
12. Popa, L.A., Burigana, C., Mandolesi, N., 2005. NewA 11, 173 (PBM).
13. Spergel, D.N. et al., 2003. ApJS 148, 175.
14. Storrie-Lombardi, L. et al., 1994. ApJ 427, L13.
15. Verde, L. et al., 2003. ApJS 148, 195.
16. White, R.L., Becker, R.H., Fan, X., Strauss, M.A., 2003, ApJ 126, 1.
17. Wyithe, J.S.B., Loeb, A., 2003. ApJ 586, 693.
18. Wyithe, J.S.B., Loeb, A., 2004. Nature 427, 815.